ROMANIAN ACADEMY
SCHOOL OF ADVANCED STUDIES OF THE ROMANIAN ACADEMY
EXACT SCIENCES DEPARTMENT

INSTITUTE OF PHYSICAL CHEMISTRY "ILIE MURGULESCU"

PhD THESIS SUMMARY

MESOSTRUCURED OXIDE NANOMATERIALS BASED ON TiO_2 WITH APPLICATION IN ENVIRONMENTAL PHOTOCATALYTIC DEPOLUTTION PROCESSES

PhD supervisor:
CP I Dr. Pârvulescu Viorica

PhD Student:
Feraru (căs.Negoescu) Daniela

BUCHAREST
2021

TABLE OF CONTENTS

Keywords: EuTi-SBA-15, PrTi-SBA-15, Ti-MCM-41, mesoporous TiO_2, property adaptation, synthesis-properties effects, TiO_2-Ag, composite systems, TiO_2-activated carbon, TiO_2/C/Ag, TiO_2/C/P/Ag, physical-chemical properties, photocatalysis, photocatalytic degradation, Brilliant Blue FCF dye, erythromycin, ciprofloxacin, gentamicin, kinetic, adsorption.

INTRODUCTION

The presence of organic and inorganic pollutants in the aquatic ecosystem poses a permanent threat to the environment and human health. Photocatalytic depollution processes offer efficient solutions for the removal of these pollutants, and the emergence of mesostructured oxide nanomaterials has generated new horizons for their approach. Thus, new photocatalytic materials were developed obtained by simple and low-cost methods, efficient, economical means of cleaning polluted water sources.

The PhD thesis presents results of the doctoral activity regarding the synthesis and characterization of TiO_2-based materials and their applications in degradation of some polluting organic compounds from water. Although the main element of these studies is titanium oxide, much studied and applied in photocatalytic reactions, 3 ways of study were approached in which novelty elements are often encountered. The first approach used methods already studied, in the team where the studies were performed, but the association of immobilized titanium oxide on mesoporous silica SBA-15 with 2 metals from the lanthanide group introduced an element of novelty.

Given that like there are numerous studies on the synthesis of mesoporous titanium oxide, a study path was approached that aimed at varying the synthesis parameters and establishing the optimal synthesis conditions necessary to obtain certain properties. The materials thus obtained present a degree of novelty in terms of properties. Another way of synthesis has even more novel elements both in terms of synthesis conditions, composition and properties of the materials obtained. Kinetics and adsorption studies also have many novelty elements.

The main objectives of the PhD experimental studies were:

- Synthesis of mono- and bimetallic oxide materials immobilized on mesoporous silica supports with ordered structure.

- Obtaining mesoporous titanium oxides with physico-chemical properties determined by varying the synthesis parameters.

- Obtaining photocatalysts by functionalization with Ag of mesoporous supports based on TiO_2.

- Obtaining the composites with TiO_2 and activated carbon.

- Obtaining the composite materials with TiO_2, activated carbon and Ag.

- Correlation of the synthesis methods and parameters with structural, textural and morphological properties as well as with photocatalytic activity.

- Study of the effects of titanium oxide surrounding and dopants on its photocatalytic properties.

- Development of new photocatalysts with high activity in degradation of some organic compounds present as impurities in wastewater.

The possibility of modeling the physico-chemical and photocatalytic properties by varying the synthesis parameters was followed and highlighted. The studies performed and the results obtained represent a challenge for obtaining new systems with photocatalytic properties and the development of new methods of photocatalytic depollution.

Thesis structure:

The first chapter presents theoretical considerations regarding the obtaining, characterization and use of the mesostructured materials based on silica funtionalized with titanium si lanthanides, mesostructured oxide nanomaterials based on TiO_2 dopped or no with activated carbon and Ag. The results obtained so far regarding the applications of TiO_2-based materials in various photodegradation reactions of organic compounds in wastewater are also presented.

The following three chapters contain their own contributions on the synthesis and properties of titanium oxide materials and their applications in the degradation of organic compounds (dyes, antibiotics) in water.

Chapter II is dedicated to obtaining mono and bimetallic oxide materials immobilized on mesoporous silica supports with an ordered porous structure. Mesostructured silica supports as MCM-41, SBA-15 were synthesized and functionalized with transition metals such as Ti, Pr, Eu. The obtained materials were tested in the photocatalytic degradation processes of dye Brilliant Blue FCF (AB) and the antibiotic erythromycin (EM).

Chapter III is structured in two parts: the synthesis and characterization of mesoporous TiO_2 oxides by sol-gel technique, using non-ionic, cationic and anionic surfactants in the presence of inorganic acids and various solvents; synthesis of TiO_2-Ag photocatalysts, by functionalizing with Ag of TiO_2 mesoporous supports. The effect of Ag doping, the morphological and structural transformations of doped TiO_2 nanopowders were investigated. The activity of the TiO_2 catalysts as well as of the obtained TiO_2-Ag materials was tested in the degradation of the dye Brilliant Blue FCF (AB) and the antibiotic ciprofloxacin (CP).

Chapter IV presents the results obtained in the synthesis, characterization and photocatalytic testing of mesoporous composite materials with TiO_2, activated carbon and Ag. It is also structured in two parts: the first presents the obtaining of composites with TiO_2 and activated carbon, having improved structural parameters and photocatalytic activity in UV light; the second part comprises the functionalization with silver of the obtained composite materials. The photocatalytic activity of the obtained catalysts was evaluated in the degradation of the dye AB and of the antibiotics CP and GM.

Thus, new photocatalytic materials were prepared, the optimal synthesis conditions were established for obtaining efficient characteristics and the parameters necessary to obtain high performances of photocatalytic degradation of some organic pollutants from wastewater were determined.

The properties of the obtained materials, based on TiO_2, were characterized by: X-ray diffraction, adsorption-desorption of N_2, scanning electron microscopy (SEM), transmission electron microscopy (TEM), diffuse reflectance UV-Vis spectroscopy, Raman and X-ray photoelectrons (XPS).

ORIGINAL RESULTS

Mono- and bimetallic photocatalysts based on TiO_2 immobilized on mesoporous silica

The large surface area, high porosity and amorphous structure of the mesoporous materials offered the possibility to incorporate the transitional metal ions within the mesopores, creating catalysts with a good photocatalytic activity. The SBA-15 mesoporous materials were synthesized by the hydrothermal method using surfactants [Chapter II.1]. SBA-15 mesoporous silica supports were functionalized with titanium by direct synthesis (samples sd) and impregnation (samples sd). New bimetallic photocatalysts LnTi-SBA-15 (where Ln = Eu or Pr) were obtained by immobilization of lanthanide ions on Ti-SBA-15 supports obtained by direct synthesis and post-synthesis (impregnation). They were tested in AB dye photodegradation reaction.

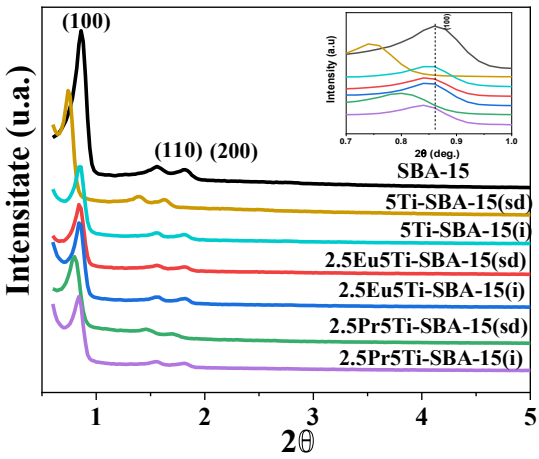

Figure 1. XRD patterns of mesoporous SBA-15, TiSBA-15 and EuTi-SBA-15 and PrTi-SBA-15 samples with 5% TiO_2 and 2.5% Eu or Pr oxide

In Figure 1 it can be seen the preservation of the ordered mesoporous structure of SBA-15 after functionalization. A shift of the reflection (100) to lower angles can be observed for all modified samples compared to the SBA-15 support (inserted graph). A less pronounced change was observed for samples 2.5EuTi-SBA-15 (i), 2.5EuTi-SBA-15 (sd) and 5TiSBA-15 (i), revealing the

preservation of the ordered mesoporous structure of silica after the incorporation of Ti andlanthanide ions.

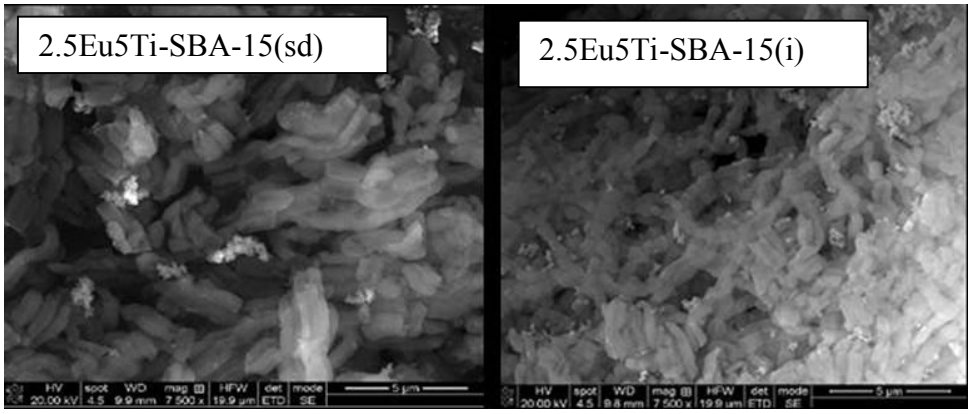

Figure 2. SEM images of samples 2.5Eu5Ti-SBA-15 (sd) and (i)

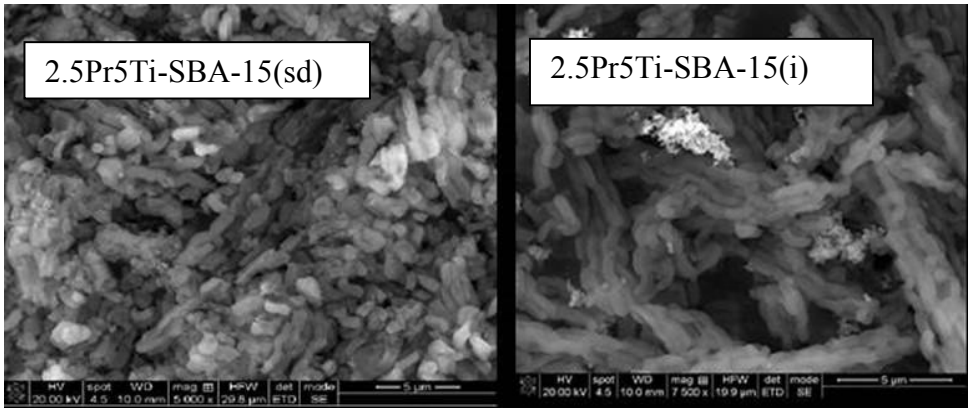

Figure 3. SEM images of samples 2.5Pr5Ti-SBA-15 (sd) and (i)

The SEM images in Figures 2 and 3 indicated a typical morphology of the SBA-15 support and the presence on the silica surface of particles that may be oxides of transition metals. Ti-SBA-15, EuTi-SBA-15 and PrTi-SBA-15 mono- and bimetallic catalysts were tested in the photocatalytic degradation of the Bright Blue FCF dye under of UV light radiation (254nm). The obtained results for the synthesized Ti-SBA-15 materials showed the increasing of the efficiency with the reaction time and reaches maximum values under acidic pH conditions. The lowest efficiency values were obtained under neutral pH conditions. The effect of the titanium immobilization method is insignificant. The acidic environment favors, first of all, the adsorption of dye molecules in the form of anionic radicals, but also the photodegradation of its molecule. In the basic medium the dye molecule is more stable and the interaction with the catalyst surface is weaker. The higher degradation efficiency was obtained for Eu samples prepared by impregnation (i) and with the lowest concentration of europium (Figure 4). The high concentrations of europium cause a decrease in the efficiency of dye degradation due to the effect on titanium oxide species. This is also evident from the UV-Vis spectra where there is a sharp decrease in absorption over the

entire wavelength range, after the addition of europium. Thus, it can be stated that the active centers are the result of the interaction of the two types of oxides, and the activation of titanium is achieved in the presence of very low concentrations of europium as dopant. Compared to the EuTi-SBA-15 photocatalyst obtained by impregnation, the degradation efficiencies were lower for the PrTi-SBA-15 (i) samples (Figure 5). This may be the result of lower band gap energy of Eu_2O_3 (2.4 eV) compared to Pr_2O_3 (3.8 ev).

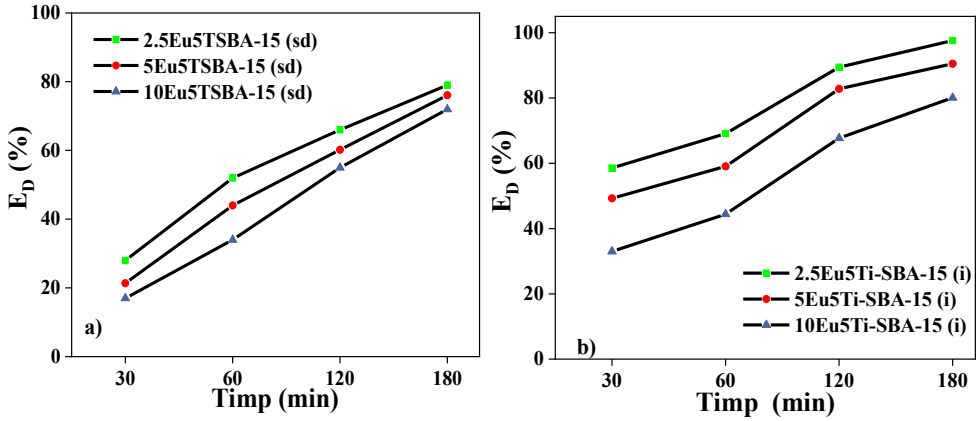

Figure 4. Dye degradation efficiencies [AB] = $1x10^{-5}$ M in the presence of Eu5Ti-SBA-15 catalysts with different concentrations obtained by direct synthesis (a) and impregnation (b)

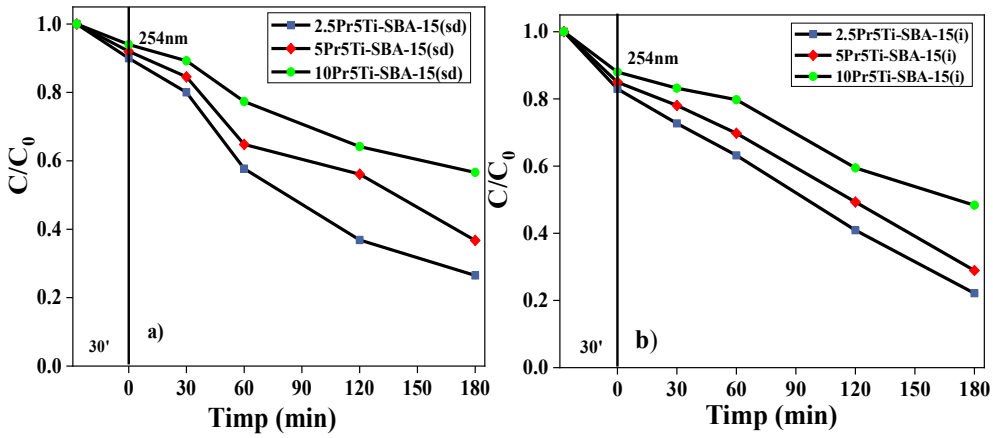

Figure 5. Photocatalytic degradation of the dye AB = $1x10^{-5}$ M in the presence of catalysts with different concentrations of Pr5Ti-SBA-15 obtained by direct synthesis (a) and impregnation (b)

The higher performance of the samples obtained by Ti impregnation is due to its dispersion on the surface, the higher absorption values at 365 nm (irradiation light), highlighted in the UV-Vis spectra, and the possible promoter effect of lanthanide oxides under higher dispersion conditions at a lower concentration (2.5%).

Photocatalysts with mesoporous TiO_2. Effects of synthesis conditions and Ag doping on photocatalytic properties and activity

The following reagents were used for the preparation of TiO_2 powders: titanium tetraisopropoxide (TTIP), titanium butoxide (TBOT) and titanium ethoxide (TEOT), cationic surfactants (cetyltrimethylammonium bromide - CTAB), anionic dodecyl sulfate SDS) and nonionic (polyoxyethylene- (23) -cetyl ether -Brij-58, polyether block copolymer - Pluronic 123, polyethylene glycol -PEG 600). Ethanol or isopropanol was used as solvent and HCl or CH_3COOH of different concentrations as acid.

All the syntheses carried out had as common steps the production of a mixture A, by dispersing the surfactant in alcohol or in acid solution, and of a mixture B, by dispersing the titanium precursor in the acid solution (hydrochloric or acetic) or in alcohol. In obtaining them, both the surfactant, acid and its concentration and the order of their addition were modified. Mesoporous titanium oxides were thus obtained, the components of the mixtures being varied. Nonionic surfactants, compared to anionic or cationic ones, led to spherical morphologies of oxide particles, higher values of surface, volume and pore diameter.

Mesoporous titanium oxides obtained by the sol-gel method in the presence of nonionic surfactants (Brij 58, PEG 600 and P123), cationic (CTAB) and anionic surfactants (SDS) showed a porous structure determined both by the surfactant and the synthesis conditions (the nature of the used inorganic acid and the solvent). Nonionic surfactants, compared to anionic and cationic ones, led to spherical morphologies of oxide particles (Figure 6), higher values of surface, volume and pore diameter. When using acetic acid, nonionic surfactants led to smaller values for these textural properties.

Following the characterization of the obtained TiO_2 powders, were selected 3 samples of titanium oxide, with larger surface area, to be doped with silver. These samples were obtained by modifying the titanium precursor (butoxide - TB sample, tetraisopropoxide - TP sample and ethoxide - TE sample) and the surfactant (CTAB - TBCH sample, Brij-58 - TPBj and TEBj samples). All these samples were obtained in the presence of 0.1 N hydrochloric acid.

X-ray diffractograms (Figure 7) do not show diffraction peaks, characteristic for crystalline silver species, which indicates that Ag, in low concentration, is well dispersed on the pore surface of the TiO_2 support. SEM images do not show significant changes in morphology (Figure 7), but show a tendency to agglomerate particles with spherical morphology due to the dilution of hydrochloric acid.

The photocatalysts TiO_2 and TiO_2-Ag were tested in the degradation reaction of the dye Brilliant Blue FCF = $1x10^{-5}$ M and the antibiotics ciprofloxacin and gentamicin in aqueous solutions, under conditions of visible range light (λ = 532 nm) and UV (λ = 254 nm).

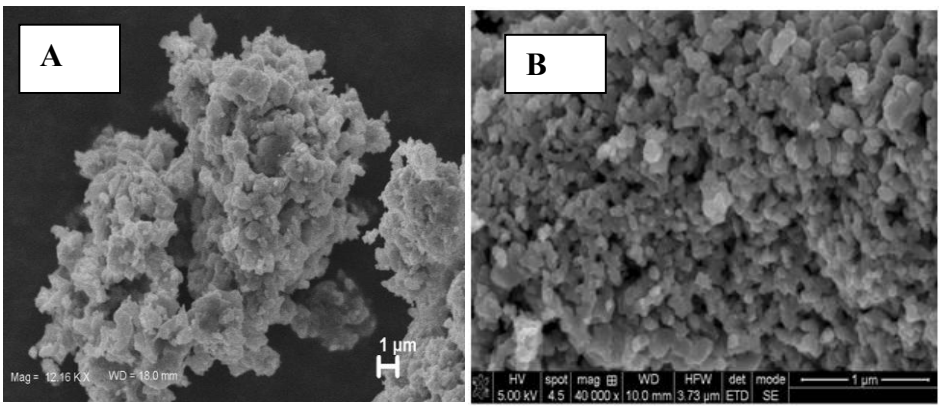

Figure 6. SEM images of TiO_2 obtained from titanium butoxide, polyethylene glycol-PEG 600 with polyether block copolymer P123 and glacial acetic acid - example TBPgPAC (A); and TiO_2 obtained from titanium tetraisopropoxide, polyoxyethylene- (23) -cetyl ether -Brij-58 and concentrated HCl - TPBjHC sample (B).

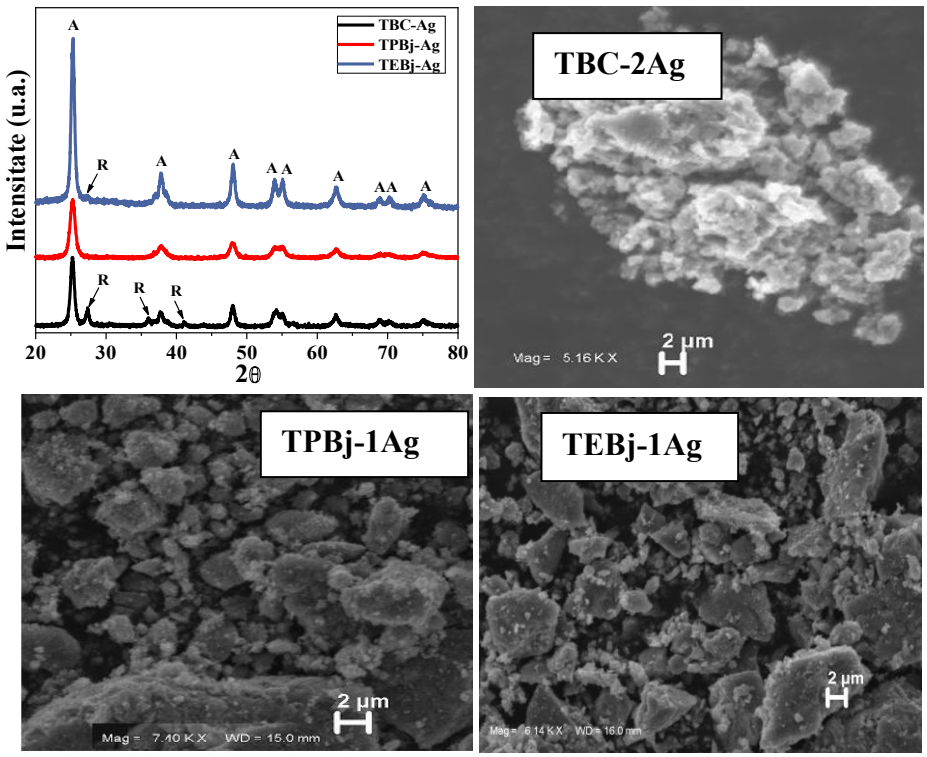

Figure 7. X-ray diffractograms and SEM images for TiO_2-Ag materials

The concentration of AB dye in the suspension decreased rapidly with the irradiation time. This indicates the efficient degradation of the dye in UV light using TiO $_2$-Ag photocatalysts (Figure 8). It was observed that the energy values of the band gap decreased from 2.95 to 2.66 eV, when the Ag content increased. The 2% silver content and the low band gap value of TBC-2Ag powder (2.66 eV) were optimal to obtain the highest degradation efficiency of AB dye under UV light irradiation.

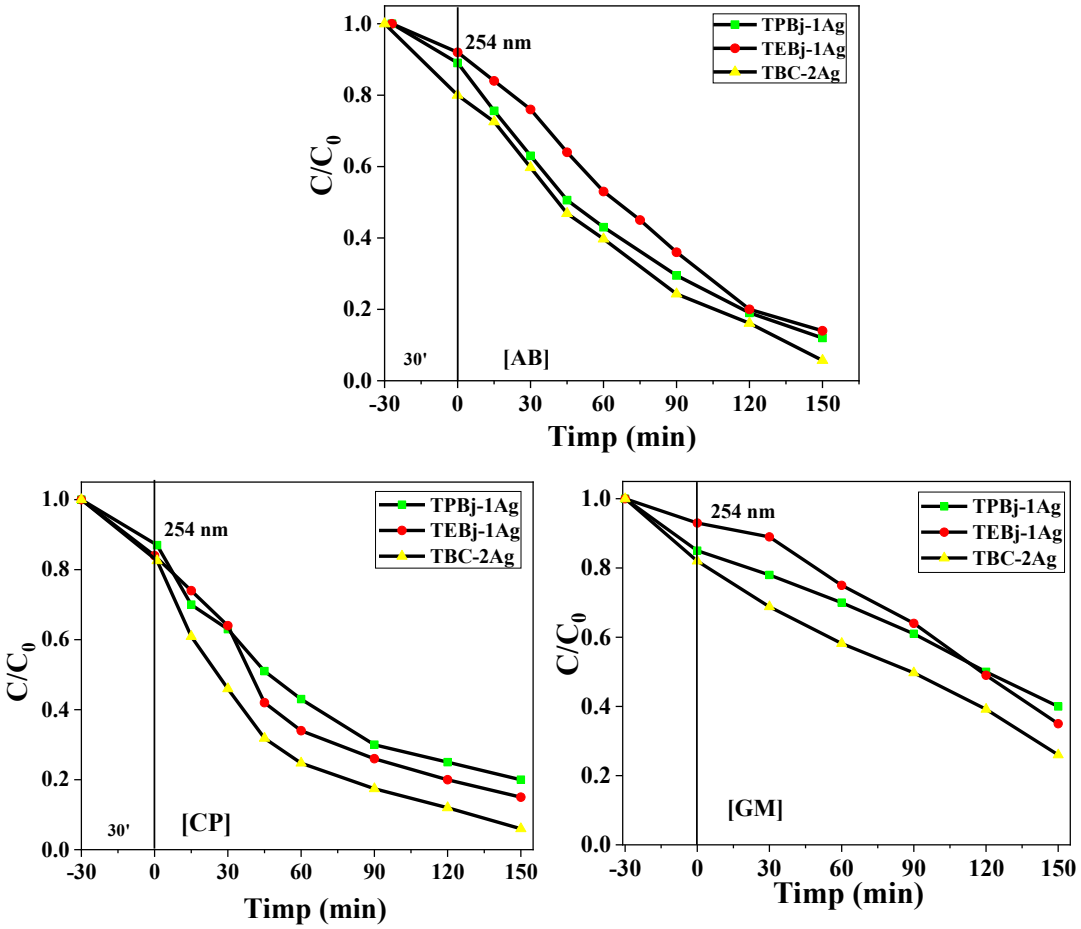

Figure 8. Photocatalytic degradation of dye AB = $1x10^{-5}$ M and antibiotics CP = 10mg / L and GM = 200mg / L in the presence of TiO_2-Ag

The results obtained (Figure 8) encouraged the use of TiO_2-Ag nanoparticles for the degradation of the antibiotics ciprofloxacin and gentamicin under UV conditions.

The improvement of the photocatalytic activity of TiO_2-Ag in dye degradation [AB] can be explained primarily by the fact that Ag nanoparticles deposited on TiO_2 act as electron traps, improving the e^--h^+ photogenerated separation and subsequent electron transfer to adsorbed O_2 acting as an electron acceptor. Second, the amount of hydroxyl radical generated is increased. The dye molecules are adsorbed on the TiO_2-Ag surface improving the transfer of photoexcited electrons from the dye molecule sensitized by visible light, in the TiO_2 conduction band subsequently increasing the electron transfer to the adsorbed O_2.

The highest dye degradation efficiencies were obtained under UV irradiation for the AB sample both before and after the silver modification. Similar results were obtained in the case of antibiotic degradation. The properties of TBC-Ag material in the degradation of Brilliant Blue FCF dye and the antibiotic ciprofloxacin, under different pH conditions using laser light (532nm) were also studied. The experimental results obtained (Figure 9) show that the degradation efficiency of the dye Brilliant Blue FCF in acid medium is about 50% in 90 minutes, compared to the neutral

medium, where a slow degradation of 18% was obtained during the 22 hours of reaction. The pH value is the major factor that influenced the speed of the photocatalytic process.

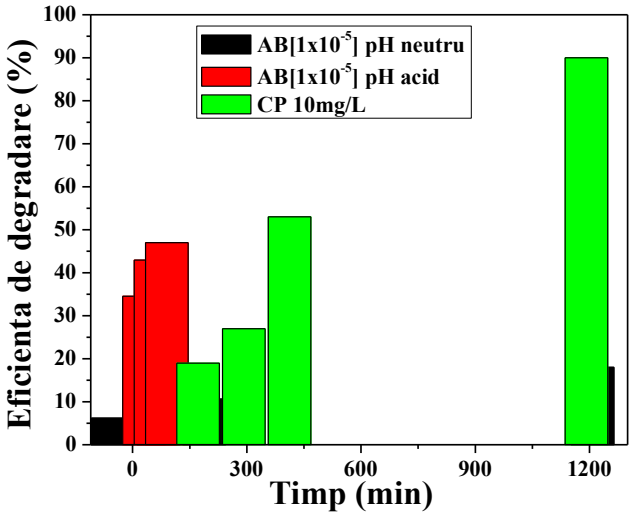

Figure 9. Degradation of dye AB = $1x10^{-5}$ M and CP = 10mg / L in the presence of TBC-2Ag and laser light (532nm)

Under UV light conditions the results of AB dye degradation were higher while in Visible light the efficiencies were lower.

Photoluminescence (PL) measurements were performed to confirm the formation of $^{\bullet}OH$ radicals on the surface of the catalysts during photocatalytic reactions. Following the irradiation of the TiO_2-Ag samples with UV light, the intensity of the emission peak increased in time, results which were in accordance with the obtained activity data.

The evaluation of these photocatalysts stability was performed in 3 successive reaction cycles. It was evidenced a higher stability for the TPBj-1Ag sample, although it did not have maximum activity in the first reaction cycle. The decrease in photodegradation efficiency was more significant after the third reaction cycle and represents about 20%.

Mesoporous composite materials with TiO_2 and activated carbon, activation with Ag and the photocatalytic applications

The composite materials were obtained by sol-gel method in the presence of titanium precursor, Brij 58 surfactant and activated carbon obtained from coffee grounds and functionalized with P by an original method [Chapter IV.7]. In order to compare the properties, the composite materials were also prepared in the absence of surfactant or by mechanical mixing of titanium oxide with activated carbon. X-ray diffraction analysis (Figure 10) indicates that all samples contain

anatase TiO_2 as the predominant phase, and the activated carbon could not be identified due to its amorphous structure.

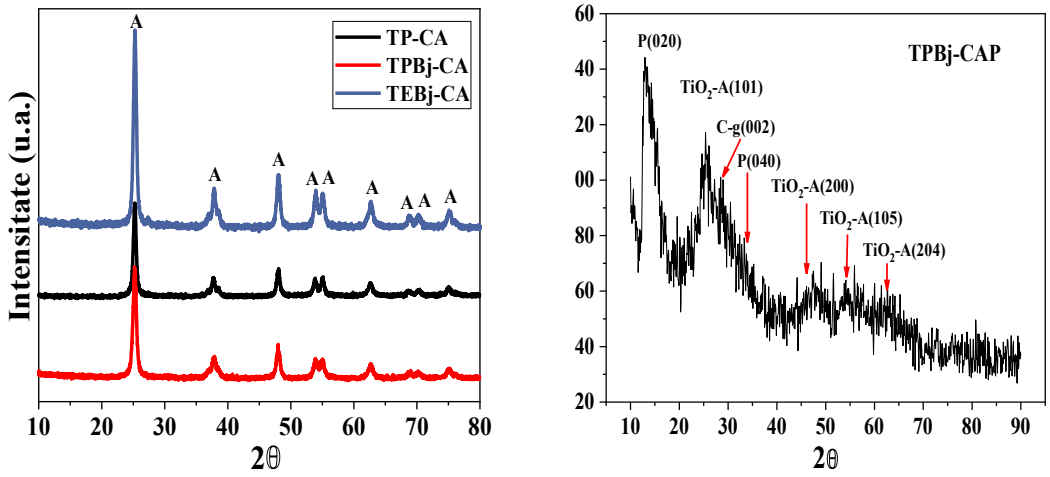

Figure 10. X-ray diffractograms of TiO_2-CA composites

The TiO_2-CAP composite material containing active phosphorus had the most significant increase of surface area and pore volume. In contrast to it, the sample without surfactant has the smallest specific surface area, as well as the lowest pore volume. The surface area of TEBj-CA sample, obtained by mechanical mixing, decreased compared to titanium oxide denoted TEBj, due to the deposition of activated carbon on the pore surface. It is observed that the use of the surfactant in sol-gel synthesis is the best choice to obtain TiO_2-CA composites with high volume and pore diameter. The high resolution XPS spectra for the C1s, Ti2p and O1s transitions of the TEBj-CA sample highlighted the presence of sp^2 and sp^3 hybridized carbon as well as its connection with oxygen. In the case of titanium, only Ti^{4+} species have been identified.

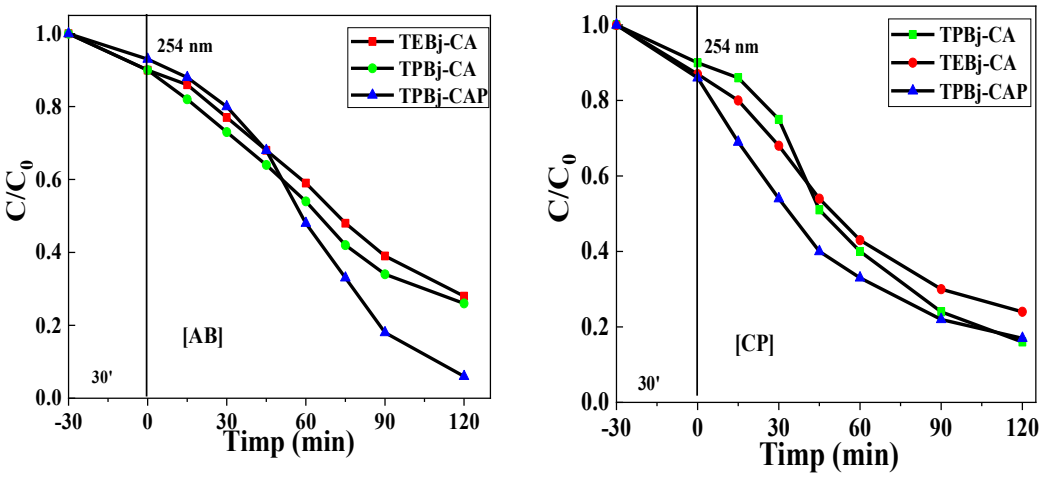

Figure 11. Time variation of photocatalytic efficiency in the presence of TiO_2-CA composite powders in the degradation of dye AB = $1x10^{-5}$ M and antibiotic CP = 10mg / L

TiO_2-CA catalysts were tested in Brilliant Blueand and ciprofloxacin photodegradation under UV irradiation (λ = 254 nm). Figure 11 show a significant decreasing of dye concentration with the irradiation time under UV light.

The composite materials TPBj-CA and TPBj-CAP (obtained by the sol-gel method) and TEBj-CA (obtained by mechanical mixing) were functionalized by impregnation with an $AgNO_3$ solution. The diffractogram of the TPBj-CAP-Ag sample, obtained in presence of the activated carbon with higher phosphourus concentration, shows a major change in the profile lines. The intensity of the diffraction lines corresponding to the anatase phase decreased and, consequently, the crystallinity of the sample decreased. The morphology of the obtained materials and their ordered porous structure were evidenced by scanning electron microscopy (SEM) and transmission electron microscopy (TEM). The SEM images (Figure 12) show a spherical morphology for all the samples.

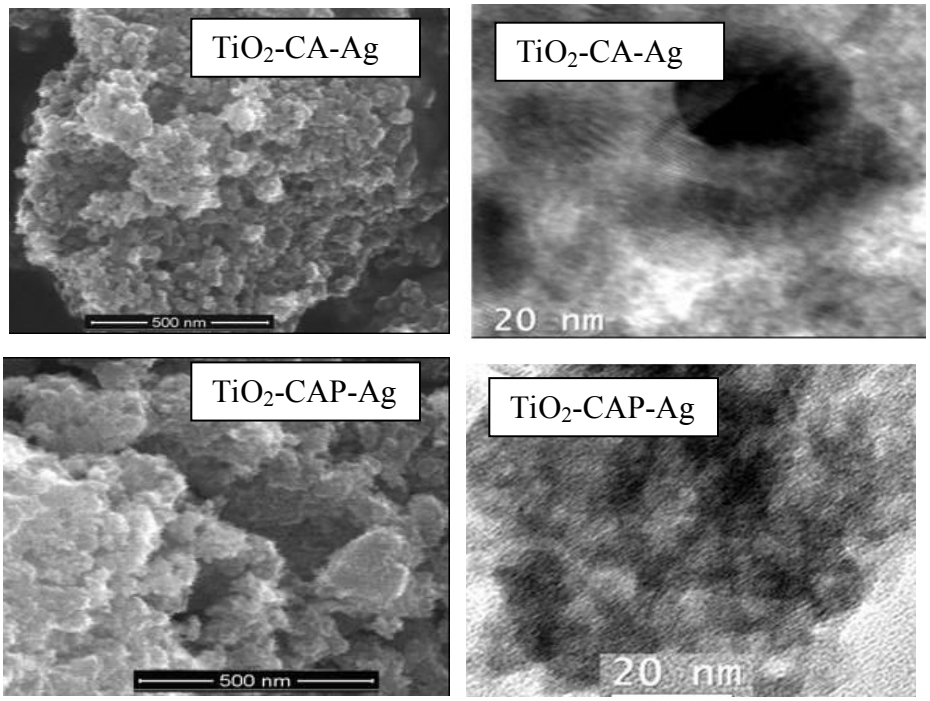

Figure 12. SEM and TEM images of composite materials

The effect of activated carbon on nanoparticle size and TiO_2 crystalline structure is better highlighted by TEM images (Figure 12). It is evident both the decrease of the particle sizes from 20-30 nm to 10-15 nm and the amorphization of the structure. Raman spectra (Figure 13) evidenced the presence of anatase, both in the sample obtained with phosphorus-free CA (TPBj-CA-Ag) and phosphorus (TPBj-CAP-Ag), which confirms the formation of anatase microcrystals in the second sample, thus completing the results obtained by X-ray diffraction.

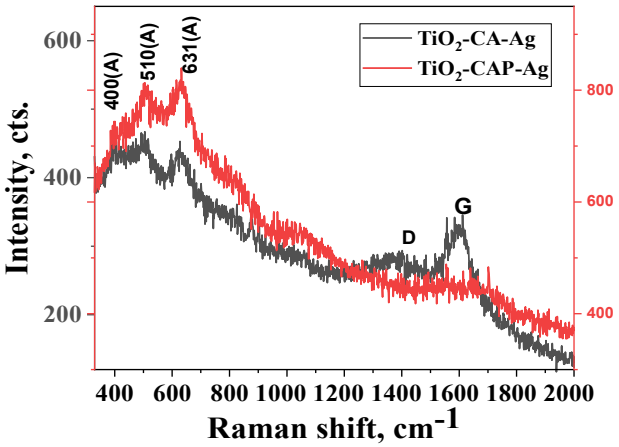

Figure 13. UV Raman spectra of TiO_2-CA-Ag and TiO_2-CAP-Ag samples with excitation line at 325 nm

UV-Vis spectra indicated for the TEBj-CA-Ag sample an absorption band in the visible light, between 420-800 nm, due to the plasmonic resonance effect of Ag nanoparticles. The presence of metallic Ag species was highlighted by XPS spectroscopy for all the obtained samples.

These composites with Ag were also tested in the photodegradation reactions of Brilliant Blue FCF dye and ciprofloxacin antibiotic from aqueous solutions. The results obtained (Figure 14) do not indicate a significant effect of Ag compared to that of activated carbon (Figure 11). The results from Figures 11 and 14 are the result of the synergistic effect of textural properties (high specific surface area), morphology of the particles that also provide a high external surface, the presence and high dispersion of carbon and phosphorus among the oxide phase of titanium oxide. In the case of ciprofloxacin degradation, the presence of activated carbon with TiO $_2$ improved the result of the photocatalytic test.

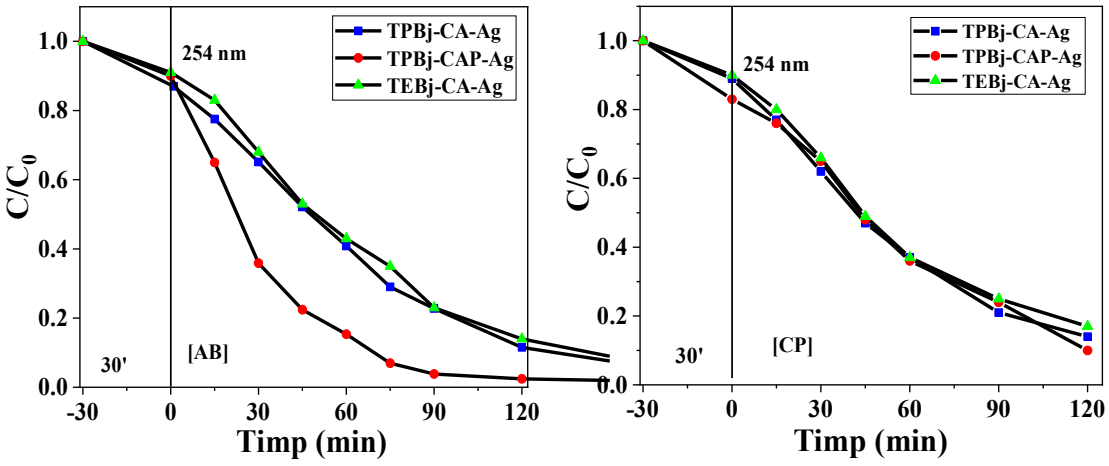

Figure. 14 Photocatalytic degradation of dye AB = $1x10^{-5}$ M in the presence of Ag composites and antibiotic CP = 10mg / L

As can be seen in Figure 14, the highest photocatalytic degradation efficiency of the Brilliant Blue dye was obtained for TPBj-CAP-Ag photocatalyst (97.53%). At the end of the photocatalytic reaction, the differences between degradation efficiencies values of the composite materials are insignificant. The results on ciprofloxacin degradation under UV light indicate high performance for all photocatalysts.

Figure 15 shows a very small decrease of degradation efficiency for the TPBj-CAP and TPBj-Ag photocatalysts after 3 reaction cycles, which indicates a very good stability of them.

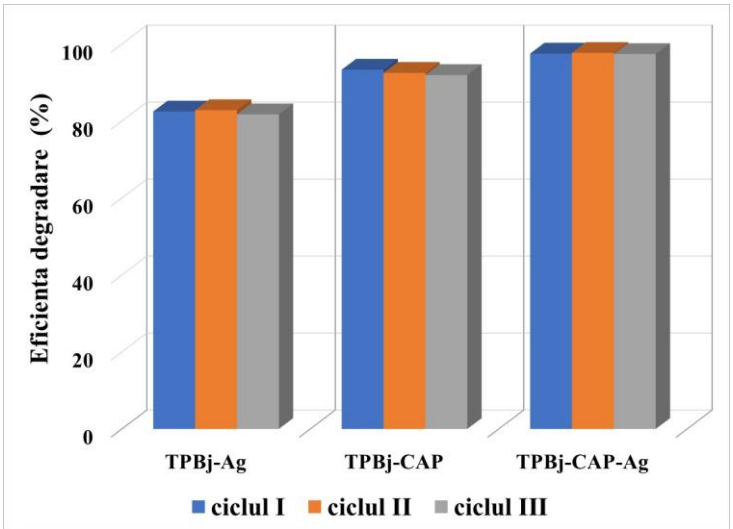

Figure 15. Recyclability test; degradation AB = $1x10^{-5}$ M under irradiation with UV light

Evaluation of antimicrobial activity revealed advanced degradation of the antibiotic cipropfloxacin in the presence of the composite photocatalyst obtained with activated carbon CAP and Ag (TPBj-CAP-Ag sample). A significant decrease of the antimicrobial activity inhibition was obtained after 5 hours of reaction, and this was in agreement with the kinetic data. The reduction to 0 of the inhibition degree, obtained after photodegradation reaction on TPBj-CAP-Ag sample, is in agreement with the activity data obtained. Kinetic studies indicated apparent 2nd order kinetics for the photocatalytic degradation reaction, and for dye adsorption the Freundlich and Dubinin-Radushkevitch isotherms indicated that physical adsorption takes place. The best correlation coefficient was obtained for the Dubinin-Radushkevitch isotherm.

FINAL CONCLUSIONS

- The research activity carried out within the PhD thesis contributed to synthesis, characterization and testing of the new materials with photocatalytic properties, useful in applications for environmental depollution.

- The configuration of the preparation conditions for these mesostructured materials allowed the establishment of optimal parameters to obtain properties of applicative interest in photocatalytic processes such as larger surface area, high porosity, narrow pore size distribution, spherical morphology, high stability.
- Comparative studies both for Ti materials supported on a mesoporous silica (MCM-41, SBA-15) and for mesoporous titanium oxides or the obtained composite materials have highlighted the effects of synthesis and composition conditions on the photocatalytic performances.
- The use of the Brilliant Blue FCF dye in evaluation of all the obtained materials activity, generated many novelty elements, this being less studied in the testing of similar materials.
- Variation of the photocatalytic reaction parameters (pH, light radiation, reaction time, and amount of catalyst) provided a lot of information on the optimal conditions. In most cases the acid pH, UV light, reaction time favored dye photocatalytic degradation.
- In most reactions of supported mono- or bimetallic photocatalysts it has been shown that the immobilization of titanium by impregnation and the lower concentration of associated metal (Eu, Pr) lead to increased photocatalytic performance.
- TiO_2 powders, obtained by the sol-gel method with anionic, cationic and non-ionic surfactants and varied synthesis parameters, were used as photocatalysts and supports, in the context of improving photocatalytic performance.
- TiO_2-Ag photocatalysts, obtained by doping TiO_2 with silver, proved to be active in degradation reaction of Blue Brilliant FCF dye, ciprofloxacin and gentamicin antibiotics under visible ($\lambda = 532$ nm) and UV ($\lambda = 254$ nm) light.
- The own method used in the activation of carbon allowed to obtain a material with high phosphorus content which proved to have a significant effect on the crystal structure, texture, particle size and photocatalytic activity of the obtained composites.
- TiO_2-activated carbon composites were prepared by adding surfactant and activated carbon obtained from coffee. The addition of activated carbon to TiO_2 materials induced a beneficial effect on Brilliant Blue FCF dye and the antibiotic ciprofloxacin photocatalytic degradation.
- TiO_2-activated carbon-Ag composites have proven to be active in Brilliant Blue FCF dye and the antibiotic ciprofloxacin degradation under UV light ($\lambda = 254$ nm).
- The obtained materials showed structural, textural, morphological properties typical of mesoporous nanomaterials. These favored formation of Ag nanoparticles on surface with a weak plasmonic effect in the visible range (400-600 nm).
- The activity tests evidenced higher performances in Brilliant Blue FCF and ciprofloxacin degradation for the composite obtained with activated carbon with higher P concentration.

- Activity data were correlated with kinetic studies, those for the determination of hydroxyl radicals and antimicrobial activity, supporting a slight increase in the activity of titanium oxide with P activated carbon by sol-gel method in the presence of surfactant (Brij 58).
- The obtained photocatalyst (TiO_2-ACP-Ag) totally degraded ciprofloxacin, the final solution no longer having antimicrobial activity.
- By recycling the photocatalysts, their high stability was highlighted after three successive cycles.
- Study of Brilliant Blue FCF dye adsorption in the presence of activated carbon, associated or not with titanium oxide, Freundlich and Dubinin-Radushkevitch isotherms indicated that physical adsorption takes place. The highest correlation coefficient was obtained for the Dubinin-Radushkevitch isotherm.

Selected Bibliography

Chapter II

1. D. Negoescu, D. C. Culita, I. Atkinson, V. Bratan, S. Petrescu, V. Parvulescu, Rev. Roum. Chim., 66 (2021) 287.
2. V. Parvulescu , B. L. Su, Catal. Today 69 (2001) 315.
3. Y. Shi, S.P. Wang, X.B. Ma, Chem. Eng. J. 166 (2011) 744.
4. K. Lin , P. P. Pescarmona, H. Vandepitte, D. Liang, G. V. Tendeloo, P. A. Jacobs, J. Catal., 254 (2008) 64.
5. M.K. Naskar, M. Eswaramoorthy, J. Chem. Sci. 120 (2008) 181.
6. L. A. Solovyov, Chem Soc. Rev. 42 (2013) 3708.
7. S. Wang, C. Ma, Y. Shi, X. Ma, Front. Chem. Sci. Eng. 8 (2014) 95.
8. V. Meynen, P. Cool, E. F. Vansant, Micropor. Mesopor. Mat. 125 (2009) 170.
9. G. N. Vassylov, Catal. Rev. Sci. Eng., 39 (1997) 209.
10. A. Wroblewska, P. Miadlicki, J. S. Nazzal, M. Sadlowski, Z. C. Koren, B. Michalkiewicz, Micropor. Mesopor. Mater. 258 (2018) 72.
11. H. Chen, Y.P. Peng, K.F. Chen, C.H. Lai, Y.C. Lin, J. Enviro. Sci. 44 (2016) 76.
12. X.N. Wei, H.L. Wang, Z.D. Li, Z.Q. Huang, H.P. Qi, W.F. Jiang, Appl. Surf. Sci. 372 (2016) 108.
13. R. Gilani, S. Joshi, V J S. Shankari, P.M. Joshna, V. Rao, IJMG 8 (1) (2017) 1.
14. D. Negoescu, P. Oancea, A. Raducan, M. Puiu, Rev. Roum. Chim., 65(2) (2021) 281.
15. C. Orbeci, R. Stanescu, D. Negoescu, V. Parvulescu, Environ. Eng. Manag. J. 16 (2017) 553.
16. R.I. Bickley, M.J. Slater, W.J. Wang, Process Saf. Environ. Prot. 83 (2005) 205.

17. M. Filip, G. Petcu, E. Anghel, S. Petrescu, B. Trica, P. Osiceanu, N. Stanica, I. Atkinson, C. Munteanu, M. Mureseanu, V. Parvulescu, Catal. Today, 366 (2021) 10-19.
18. L. Yang, Z. Jiang, S. Lai, C. Jiang, H. Zhong, Int. J. Chem. Eng. (2014) 1.
19. C. Lin, K. Tao, H. Yu, D. Hua, S. Zhou, Catal. Sci. Technol. 4 (2014) 4010.
20. T. Olejnik, S. P.Patkowska, A. Lesiuk, J. Ryczkowski, Pol. J. Chem. Technol., 18 (2016) 30.
21. T. Diaconu, M. Ciobanu, G. Petcu, D. Culita, S. Preda, J. P. Cusu, M. Mureseanu, V. Parvulescu , Rev. Roum. Chim., 63 (2018) 467.
22. M. Thommes, Chem. Ing. Technik. 82 (2010) 1059.
23. Y.J. A. Silva, R. Nava, V. H. Morales, S.A. M. Sanchez, M.L.G. Herrera, B. Pawelec, Appl. Catal. B: Environ. 110 (2011) 108
24. T. Benamor, L. Vidal, B. Lebeau, C. Marichal, Micropor. Mesopor. Mater., 153 (2012) 100.
25. K.M. Choi, T. Yokoi, T. Tatsumi, K. Kuroda, J. Mater. Chem. A, 1 (2013) 2485.
26. M.A. Malecka, L. Kepinski, J. Alloy Compd. 430 (2007) 282.
27. K. Naeem, O. Feng, J. Env. Sci., 21 (2009) 527.
28. J. Li, J. Fenga, W. Yan, Appl. Surf. Sci., 279 (2013) 400.

Chapter III

1. F. Z. Haque, R.Nandanwar, P. Singh, Optik 128 (2017) 191.
2. J. H. Ku, H. S. Kim, M. H. Cho, J. Y. Ahn, S. H. Kim, Chem. Phys. Lett. 715 (2019) 134.
3. J. Zhou, B. Song, G. Zhao, G. Han, Nano. Res. Lett. 7 (2012) 7.
4. F. Sayilkan, M. Asilturk, H. Sayilkan, Y. Onal, M. Akarsu, E. Arpac, Turk J. Chem 29 (2005) 697.
5. M. Pelaez, N. T. Nolan, S. C. Pillai, M. K. Seery, P. Falaras, A. G. Kontos, P. S.M. Dunlop, J.W.J. Hamilton, J.A. Byrne, K. O'Shea, M. H. Entezari, D. D. Dionysiou, Appl. Catal. B: Environ. 125 (2012) 331.
6. A. M. Sescu, L. Favier, D. Lutic, N. S. Donoso, G. Ciobanu, M. Harja, Water 13 (2021) 19.
7. Z. Sarteep, A. E. Pirbazari, M. A. Aroon, J.Water Environ. Nano. 1 (2016) 135.
8. M. K. Seery, R. George, P. Floris, S.C. Pillai, J. Photochem. Photobiology A: Chem., 189 (2007) 258.
9. K. S. W. Sing, D. H. Everett, R. A. W. Haul, L. Moscou, R. A. Pierotti, J. Rouquerol, T. Siemieniewska, Pure & App. Chem. 57 (1985) 603.
10. E. T. Wahyuni, R. Roto, Silver Nanoparticle Incorporated Titanium Oxide for Bacterial Inactivation and Dye Degradation, Titanium Dioxide - Material for a Sustainable Environment, IntechOpen 2018.
11. K. H. Leong, B. L. Gan, S. Ibrahim, P. Saravanan, Appl. Surf. Sci. 319 (2014) 128.

12. F. Wu, X. Hu, J. Fan, E. Liu, T. Sun, L. Kang, W. Hou, C. Zhu, H. Liu, Plasmonics 8 (2013) 501.
13. V. Amendola, O.M. Bakr, F. Stellacci, Plamonics 5 (2010) 85.
14. S. Linic, P. Christopher, D. B. Ingram Nature Materials 10 (2011) 911.
15. T. Handoko, N.G. Moustakas, T. Peppel, A. Springer, F.E. Oropeza, A. Huda, M. D. Bustan, B. Yudono, F. Gulo, J. Strunk, Catalysts 9 (2019) 323.
16. K. Awazu, M. Fujimaki, C. Rockstuhl, J. Tominaga, H. Murakami, Y. Ohki, N. Yoshida, T. Watanabe. J Am. Chem. Soc. 130 (2008) 1676.
17. C. Chen, X. F. Leic, M. Z. Xue, J. Chem. Res. 41 (2017) 475.
18. G. Oliveiri, G. Ramis, V.S. Escribano, J. Mater. Chem. 12 (1993) 1239.
19. M.A. Rauf, M.A. Meetani, S. Hisaindee, Desalination 276 (2011) 13.
20. N. Sobana, M. Muruganadham, M. Swaminathan, J. Mol. Catal. A: Chem. 258 (2006) 124.
21. A. R. Silva, P. M. Martins, S. Teixeira, S. A. C. Carabineiro, K. Kuehn, G. Cuniberti, M. M. Alves, S. Lanceros-Mendezagh, L. Pereira, RSC Adv. 6 (2016) 95494.
22. M. M. Baneshi, S. Jahanbin, A. Mousavizadeh, S. A. Sadat, A. R. Shirazi, H. Biglari, Pol. J. Environ. Stud. 27 (2018) 1433.
23. S. Esplugas, D.M. Bila, L.G.T Krause, M. Dezotti, J. Haz. Mat. 149 (2007)-631.
24. U. J. Rivera, G. J. Prados, M. Sánchezpolo, M. F. García, I. T. Bautista, J. Haz. Mat. 170 (2009) 298.
25. S. Kochuveedu, Y. H. Jang , D. H. Kim, Chem. Soc. Rev. 42 (2013) 8467.
26. M. Mureseanu, M. Filip, S. Somacescu, A. Baran, G. Carja, V. Parvulescu , Appl. Surf. Sci. 444 (2018) 235.

Chapter IV

1. M. Munner, M. Qamar, M. Saquib, D.W. & Bahnemann, Chemosphere, 61 (2005) 457.
2. H. Chen, Z. Sun, W. Ni, K.C. Woo, H.Q.Lin, L. Sun, C. Yan, J. Wang, Small 5, (2009**)** 2111.
3. A. M. Aljeboree, A. N. Alshirifi, A. F. Alkaim, Arab. J. Chem. (2017) 10, S3381–S3393.
4. I. Matos, M. Bernardo, I. Fonseca, Catal. Today 285 (2017) 194.
5. M. Molina-Sabio, R. Reinoso F., Colloid. Surf., A 241 (2004) 15.
6. L. Giraldo, J. C. Moreno-Pirajan, J. Chem. 9 (2012) 938.
7. D. Negoescu, I. Atkinson, M. Gherendi, D. C. Culiţa, A. Baran, S. Petrescu, B. Trică, R. Ionescu, D. Pelinescu, V. Bratan, V. Parvulescu ”Brij 58 assited Ag/P/C/TiO_2 efficient photocatalysts for water organic pollutants” trimis la publicat J. Alloys Compounds.
8. S. M. Lamine, C. Ridha, H. M. Mahfoud, C. Mouad, B. Lotfi, A. H. Al-Dujaili, Energy Procedia 50 (2014) 393.

9. B. S. Girgis, Y. M. Temerk, M. M. Gadelrab, I. D. Abdullah, Carbon Sci. 8 (2007) 95.
10. J.M Rosas, J. Bedia, J. R. Mirasol, T. Cordero, Fuel 88 (2009) 19.
11. Y.J. Xu, Y. Zhuang, X. Fu, J. Phys. Chem. 114 (2010) 2669.
12. B. Xing, C. Shi, C. Zhang, G. Yi, L. Chen, H. Guo, G. Huang, J. Cao, J. Nanomater., 1- 10 (2016).
13. T. Ohsaka, F. Izumi, Y. Fujiki, J. Raman Spectrosc., 7 (6) (1978) 321.
14. S.C. Chan, M.A.Barteau, Langmuir, 21 (2005) 5588.
15. M. Tudose, E. Anghel, D.C. Culita, S. Somacescu, J. Calderon, V. Tecuceanu, F.D. Dumitrascu, O. Dracea, M. Popa, L. Marutescu, C. Bleotu, C. Curutiu, M.C. Chifiriuc, Appl. Surf. Sci. 471 (2019) 553.
16. S. A. Hassan, R. A. El-Salamony, Can. Chem. Trans., 2 (2014),
17. L. Han, Y. Gao, X. Gao, W. Gong, H. Wang, Web of Conferences 245, 02039 (2021).
18. A. Berez, G. Schäfer, F. Ayari, M. Trabelsi-Ayadi, Int. J. Environ. Sci. Technol. 13 (2016) 1625.
19. J. Bedia, M. P. Garzón , A. G. Avilés, J. J. Rodriguez, C. Belver, J. Carbon Research 4 (2018) 63.
20. H. A. AL-Aoh, R. Yahya, M. J. Maah, M. R. Bin Abas, Desal. Water Treat. (2013) 1.